Low-frequency electrostatic waves in self-gravitating dusty plasmas with dust-ion collisions

G. Jacobs,[1] V. V. Yaroshenko,[2,*] and F. Verheest[1]
[1]*Sterrenkundig Observatorium, Universiteit Gent, Krijgslaan 281, B-9000, Gent, Belgium*
[2]*Katholieke Universiteit Leuven, Celestijnenlaan 200B, B-3001 Heverlee, Belgium*
(Received 8 February 2002; published 16 August 2002)

The influence of dust-ion collisions on low-frequency modes in a self-gravitating dusty plasma is studied. The stability of the system is easily determined using elementary principles of rootlocus theory. It shows that collisions between ions and dust grains do not change the criteria for gravitational collapse at any value of their collision frequency, but diminish the growth rate of unstable dusty plasmas. Moreover, the rootlocus plots visualize qualitatively the evolution of the real frequencies and damping decrements of the dust-acoustic and ion-acoustic modes as the dust-ion collision frequency increases.

DOI: 10.1103/PhysRevE.66.026407 PACS number(s): 52.27.Lw, 52.35.Fp, 02.30.Yy

I. INTRODUCTION

Dusty plasmas are ensembles of traditional plasma components and dust particles. In space applications these dust particles display an incredible variety in size, shape, and composition, thus making the features of dusty plasmas much more complex than those of traditional electron-ion plasmas. The surge of interest in dusty plasmas is partly due to the presence of ultralow-frequency waves [1–4], arising as a consequence of the very heavy nature of the charged dust grains. This research area was stimulated by the prediction of the dust-acoustic wave by Rao *et al.* [1], just over a decade ago. The massive dust grains also induce self-gravitational interactions that modify collective modes and lead to a gravitational collapse of sufficiently large astrophysical dusty plasmas [5].

We now study low-frequency electrostatic waves in self-gravitating dusty plasmas with charged dust grains. Earlier work in self-gravitating dusty plasmas usually relied upon a collisionless model [5], while other authors included collisions but neglected self-gravitation [6–10]. On the other hand, Shukla and Verheest [11] studied self-gravitating collisional dusty plasmas but neglected the possibly important ion inertia. The model used in our paper deals with a dusty plasma without neutrals and only retains the dust-ion collisions, as this is then the dominant collision mechanism. This model proves suitable for application of the rootlocus method, a mathematical tool for stability analysis that also allows a visual inspection of the influence of dust-ion collisions on the ion-acoustic and dust-acoustic modes.

The paper is organized as follows. In Sec. II the basic equations are recalled; next, in Sec. III we derive the general dispersion relation and discuss it for the collisionless limit and for small collision frequencies. In Sec. IV, the stability analysis is given and the rootlocus method is applied, in order to show the modification of the ion- and dust-acoustic modes due to inclusion of the collisional mechanism between the ions and charged dust grains. At the end, Sec. V contains our conclusions.

*Present address: Max-Planck Institute for Extraterrestrial Physics, Postfach 1312, D-85741 Garching, Germany.

II. GENERAL FORMALISM

The model we investigate is a collisional dusty plasma consisting of electrons, ions, and charged dust grains where only dust-ion collisions are retained. The electrostatic waves under consideration propagate along the x axis and their wave period is assumed to differ considerably from the dust charge fluctuation time, so that we can treat the dust charges as effectively constant, also because we are not considering too large charges for which crystalline effects might come into play. The phase speed of the waves is much smaller than the thermal speeds of the electrons and therefore the electrons are treated as being Boltzmann distributed:

$$n_e = n_{e0}\exp\left(\frac{e\psi_E}{k_B T_e}\right). \tag{1}$$

Our basic equations further include the continuity equations

$$\frac{\partial n_i}{\partial t} + \frac{\partial}{\partial x}(n_i v_i) = 0, \tag{2}$$

$$\frac{\partial n_d}{\partial t} + \frac{\partial}{\partial x}(n_d v_d) = 0, \tag{3}$$

and the equations of motion for the ions and dust particles,

$$\frac{\partial v_i}{\partial t} + v_i\frac{\partial v_i}{\partial x} + \frac{q_i}{m_i}\frac{\partial \psi_E}{\partial x} + \frac{\partial \psi_G}{\partial x} + \frac{v_{Ti}^2}{n_i}\frac{\partial n_i}{\partial x} + \nu_{id}(v_i - v_d) = 0, \tag{4}$$

$$\frac{\partial v_d}{\partial t} + v_d\frac{\partial v_d}{\partial x} + \frac{q_d}{m_d}\frac{\partial \psi_E}{\partial x} + \frac{\partial \psi_G}{\partial x} + \frac{v_{Td}^2}{n_d}\frac{\partial n_d}{\partial x} + \nu_{di}(v_d - v_i) = 0, \tag{5}$$

where

$$\nu_{di} = \frac{m_i n_{i0}}{m_d n_{d0}}\nu_{id}. \tag{6}$$

Different species are labeled with indices α, their densities, fluid velocities, charge, and mass are, respectively, denoted

by n_α, v_α, q_α, and m_α. The thermal velocities enter as $v_{T\alpha}$ while ν_{id} and ν_{di} are the collision frequencies. The electric ψ_E and gravitational potentials ψ_G can be found from the Poisson equations

$$\frac{\partial^2 \psi_E}{\partial x^2} = \frac{1}{\varepsilon_0}(n_e e - n_i q_i - n_d q_d), \tag{7}$$

$$\frac{\partial^2 \psi_G}{\partial x^2} = 4\pi G(m_i n_i + m_d n_d). \tag{8}$$

III. DISPERSION RELATION

Assuming the perturbations to be proportional to exp $[-i\omega t + ikx]$, we obtain after linearizing Eqs. (1)–(8) the dispersion relation

$$\left[\omega\left(\omega + i\nu_{id}\frac{\omega_{Ji}^2}{\omega_{Jd}^2}\right) - k^2 v_{Td}^2 + \omega_{Jd}^2 - A\omega_{pd}^2\right] \times [\omega(\omega + i\nu_{id}) - k^2 v_{Ti}^2 + \omega_{Ji}^2 - A\omega_{pi}^2] = \left[A\omega_{pi}\omega_{pd} - \omega_{Ji}\omega_{Jd} + i\omega\nu_{id}\frac{\omega_{Ji}}{\omega_{Jd}}\right]^2. \tag{9}$$

For convenience, A is an abbreviated notation and stands for

$$A = \left(1 + \frac{1}{k^2\lambda_{De}^2}\right)^{-1}. \tag{10}$$

Here $\lambda_{D\alpha} = (\varepsilon_0 k_B T_\alpha / n_{\alpha 0} q_\alpha^2)^{1/2}$, $\omega_{p\alpha} = (n_{\alpha 0} q_\alpha^2/\varepsilon_0 m_\alpha)^{1/2}$, and $\omega_{J\alpha} = (4\pi G n_\alpha m_\alpha)^{1/2}$ are, respectively, the Debye length, the plasma, and Jeans frequencies of species α. For later use, we also introduce the global plasma Debye length $\lambda_D^{-2} = \lambda_{De}^{-2} + \lambda_{Di}^{-2}$. For cold dust without dust-ion collisions and neglecting ω_{Ji}, Eq. (9) is equal to Eq. (27) of Meuris *et al.* [12], but without streaming. Without self-gravitation, with $k^2\lambda_{De}^2 \ll 1$ and $Z_i = 1$, $q_d = -eZ_d$, Eq. (9) can be written as

$$\omega^4 - k^2[\lambda_{De}^2(\omega_{pi}^2 + \omega_{pd}^2) + v_{Ti}^2]\omega^2 + k^4\lambda_{De}^2\omega_{pd}^2 v_{Ti}^2 + i\nu_{di}\omega\left\{\omega^2 - k^2\left[v_{Ti}^2 + \lambda_{De}^2\omega_{pi}^2\left(1 - \frac{n_{d0}}{n_{i0}}Z_d\right)\right]\right\} = 0, \tag{11}$$

which equals Eq. (21) of D'Angelo [6] if one sets there $\tau_L = \infty$ and $\alpha = 0$. In the latter paper, figures of growth rates for different plasma and dust parameters can be found. When substituting $\omega = i\Omega$ in the dispersion relation (9), we obtain a quartic equation with real coefficients, viz.,

$$P(\Omega,0) + \nu_{id}\Omega[\Omega^2 - \Lambda] = 0, \tag{12}$$

where the biquadratic equation $P(\Omega,0) = 0$ is the collisionless dispersion relation

$$P(\Omega,0) = [\Omega^2 + A\omega_{pd}^2 + k^2 v_{Td}^2 - \omega_{Jd}^2] \times [\Omega^2 + A\omega_{pi}^2 + k^2 v_{Ti}^2 - \omega_{Ji}^2] - [A\omega_{pi}\omega_{pd} - \omega_{Ji}\omega_{Jd}]^2, \tag{13}$$

and since naturally $\omega_{Ji} \ll \omega_{Jd}$, we can calculate Λ as

$$\Lambda = \omega_{Jd}^2 - k^2 v_{Td}^2\left(1 + \frac{n_{i0}T_i}{n_{d0}T_d}\right) - A\omega_{pd}^2\left(1 + \frac{n_{i0}Z_i}{n_{d0}Z_d}\right)^2. \tag{14}$$

Here the following equalities are valid (for negatively charged grains), viz., $n_{i0}Z_i = n_{e0} + n_{d0}Z_d > n_{d0}Z_d$ and $n_{i0}T_i \gg n_{d0}T_d$. Further on, the full dispersion relation (12) is denoted as $P(\Omega, \nu_{id}) = 0$.

For dusty plasmas with very heavy dust particles so that $(1 + n_{i0}Z_i/n_{d0}Z_d)\omega_{pd} < \omega_{Jd}$ is satisfied, it shows that Λ is always positive. On the other hand, for lighter dust species that satisfy $(1 + n_{i0}Z_i/n_{d0}Z_d)\omega_{pd} > \omega_{Jd}$, the sign of Λ depends on the wave number. For a dusty plasma with cold dust particles that follow the latter inequality, we introduce the wave number k_Λ as

$$k_\Lambda^2 = \frac{\omega_{Jd}^2}{\left[\left(1 + \frac{n_{i0}Z_i}{n_{d0}Z_d}\right)^2\omega_{pd}^2 - \omega_{Jd}^2\right]\lambda_{De}^2} \tag{15}$$

and we see that Λ is negative for $k > k_\Lambda$ and positive for $k < k_\Lambda$. We assume $k^2\lambda_D^2 \simeq k^2\lambda_{Di}^2 \ll 1$, and hence it is clear that $k_\Lambda < \omega_{Jd}/c_{da}$, with $c_{da} = \lambda_D\omega_{pd}$ being the dust-acoustic speed. It will become clear that the dust-ion collisions exert a different influence on wave number regions separated by k_Λ.

A. Collisionless dispersion relation

The discriminant of $P(\Omega,0) = 0$, the collisionless dispersion relation, is

$$D^* = [A(\omega_{pi}^2 - \omega_{pd}^2) + k^2(v_{Ti}^2 - v_{Td}^2) - (\omega_{Ji}^2 - \omega_{Jd}^2)]^2 + 4(A\omega_{pi}\omega_{pd} - \omega_{Ji}\omega_{Jd})^2 \geqslant 0, \tag{16}$$

implying that both roots in Ω^2, viz., r_{ia} and r_{da},

$$r_{ia,da} = -\frac{1}{2}[A(\omega_{pi}^2 + \omega_{pd}^2) + k^2(v_{Ti}^2 + v_{Td}^2) - (\omega_{Ji}^2 + \omega_{Jd}^2) \pm \sqrt{D^*}], \tag{17}$$

are real; here, r_{ia} corresponds to the $+$ sign and r_{da} with the $-$ sign. Obviously $r_{ia} \gg r_{da}$ and therefore the roots of $P(\omega,0) = 0$ can be approximated as

$$r_{ia} \simeq -A\omega_{pi}^2 - k^2 v_{Ti}^2, \tag{18}$$

$$r_{da} \simeq \omega_{Jd}^2 - k^2(c_{da}^2 + v_{Td}^2), \tag{19}$$

and this makes it clear that r_{ia} and r_{da} indeed represent the ion-acoustic and the dust-acoustic branches, respectively, of

the dispersion relation. While r_{ia} is always negative, the sign of r_{da} switches at the critical wave number

$$k_{cr}^2=\frac{\omega_{Jd}^2}{c_{da}^2+v_{Td}^2}\simeq\frac{\omega_{Jd}^2}{c_{da}^2}; \tag{20}$$

thus, we have $r_{da}\leqslant 0$ if $k\geqslant k_{cr}$ and vice versa $r_{da}>0$ if $k<k_{cr}$ [3,5].

We pay extra attention to a dusty plasma with negligible self-gravitational interactions, and in that special case we obtain

$$r_{ia}\cdot r_{da}=k^2[k^2v_{Ti}^2v_{Td}^2+A(\omega_{pi}^2v_{Td}^2+\omega_{pd}^2v_{Ti}^2)]\geqslant 0 \tag{21}$$

and we can conclude that in this case $r_{da}\leqslant 0$ holds.

We now rewrite Eq. (12) in the form

$$(\Omega^2-r_{ia})(\Omega^2-r_{da})+\nu_{id}\Omega(\Omega^2-\Lambda)=0, \tag{22}$$

as it is more compact and practical for further analysis. Note that $r_{da}-\Lambda$ is always positive because

$$r_{da}-\Lambda>\frac{1}{2}[\sqrt{D^*}-\omega_{Jd}^2-A(\omega_{pi}^2-\omega_{pd}^2)-k^2(v_{Ti}^2-v_{Td}^2)]>0. \tag{23}$$

B. Small and large collision frequencies

Starting from Eq. (22), series expansions in ν_{id} for r_{ia}, r_{da}, and Λ can easily be determined. For small ν_{id}, we calculate for $\Omega\simeq\sqrt{r_{ia}}$ up to first order,

$$\Omega=\sqrt{r_{ia}}-\frac{\nu_{id}}{2}\frac{(r_{ia}-\Lambda)}{(r_{ia}-r_{da})}\simeq\sqrt{r_{ia}}-\frac{\nu_{id}}{2}, \tag{24}$$

because $|r_{da}|,|\Lambda|\ll|r_{ia}|$. Similarly, for $\Omega\simeq\sqrt{r_{da}}$, we approximate to first order

$$\Omega=\sqrt{r_{da}}-\frac{\nu_{id}}{2}\frac{(r_{da}-\Lambda)}{(r_{da}-r_{ia})}\simeq\sqrt{r_{da}}+\frac{\nu_{id}}{2}\frac{(r_{da}-\Lambda)}{r_{ia}} \tag{25}$$

and we can see that the second term on the right-hand side is always real.

For negative Λ the roots (in Ω) of $P(\Omega,\pm\infty)=0$ are $\pm i\sqrt{|\Lambda|}$ and 0. Here, we can expand for large ν_{id} and so calculate for $\Omega\simeq i\sqrt{|\Lambda|}$ the first terms of the series expansion in the small parameter ν_{id}^{-1},

$$\Omega=i\sqrt{|\Lambda|}+\frac{(r_{ia}+|\Lambda|)(r_{da}+|\Lambda|)}{2\nu_{id}|\Lambda|}\simeq i\sqrt{|\Lambda|}+\frac{r_{ia}(r_{da}+|\Lambda|)}{2\nu_{id}|\Lambda|}. \tag{26}$$

The expressions for positive Λ are obviously very similar and not given here. Finally, for $\Omega\simeq 0$ we obtain

$$\Omega\simeq\frac{r_{ia}r_{da}}{\nu_{id}\Lambda}. \tag{27}$$

Equations (26) and (27) are mentioned here because the semianalytical method, which is used in the next section, requires a mathematical solution for infinite collision frequencies. We emphasize that in these equations, the collision frequency is treated as a purely mathematical parameter. After all, the mathematical solutions for very large collision frequencies may not be physically meaningful, as in that situation our basic equations are not valid anymore. However, it is imperative to realize that the validity for realistic values of the collision frequency is not affected when we extend the use of the parameter ν_{id} beyond its physical relevance. Basically, we calculate the solutions for all values of the collision frequency; afterwards, the solutions for very large ν_{id} can be discarded.

IV. ROOTLOCUS METHOD APPLIED ON STABILITY ANALYSIS

Equation (22) is a full quartic equation in Ω that also contains a parameter ν_{id} and has trivial solutions $(\Omega,\nu_{id})=(0,\infty)$, $(\pm i\sqrt{|r_{ia}|},0)$, $(\pm\sqrt{r_{da}},0)$, and $(\pm\sqrt{\Lambda},\infty)$. Note that some of these trivial roots in Ω can be purely imaginary but there are no other purely imaginary roots for finite, nonzero values of the collision frequency, except for the special cases $r_{da}=-\Lambda>0$ and $r_{da}=0$. Because $|r_{ia}|\gg|r_{da}|$, we can also see that

$$\Omega=-\sqrt{-r_{ia}}, \tag{28}$$

with corresponding

$$\nu_{id}=2\frac{r_{ia}+r_{da}}{r_{ia}+\Lambda}\sqrt{-r_{ia}}\simeq 2\sqrt{-r_{ia}}, \tag{29}$$

is a real and negative solution of the dispersion relation; moreover, it is a double root.

Since Eq. (22) can be written as $D(\Omega)+\nu_{id}N(\Omega)=0$, where $N(\Omega)$ and $D(\Omega)$ are polynomials in the complex variable Ω and with real coefficients, one can always make a so called rootlocus plot [13]. This plot shows how the roots of the dispersion relation (22) move in the complex plane as ν_{id} increases. The roots of $N(\Omega)$ are called the zeros, while the roots of $D(\Omega)$ are called poles. Because ν_{id} is a positive parameter, the loci of the solutions of the dispersion relation will originate in the poles and terminate in the zeros if one increases ν_{id}, starting from zero towards infinity. Without actually plotting the rootlocus, we can already derive some of its properties by just studying the rational function $N(\Omega)/D(\Omega)$.

The coefficients of Eq. (22) are real, and this is eventuated in one of the general properties of rootlocus plots; viz., they are symmetrical with respect to the real axis.

Stable solutions require Ω to have a negative real part as $\omega=i\Omega$; therefore, all roots located in the right half of the complex plane can be recognized as unstable solutions.

For the dispersion relation (22), the rootlocus plot will cross the imaginary axis only in poles or zeros because for $\nu_{id}\neq 0$ and $\nu_{id}\neq\infty$ there are no purely imaginary roots, as mentioned before. This is an important remark for the determination of the stability of the system.

We can easily deduct which parts of the real axis correspond with sets of solutions (Ω, ν_{id}) of Eq. (22) and are thus part of the rootlocus plot. Therefore we rewrite $D(\Omega) + \nu_{id} N(\Omega) = 0$ as

$$1 + \nu_{id} \frac{\Pi_{i=1}^{q} (\Omega + z_i)}{\Pi_{i=1}^{p} (\Omega + p_i)} = 0, \tag{30}$$

where p_i stand for the poles, z_i for the zeros, and p and q for the number of poles and zeros, respectively. Suppose a certain Ω is real; then,

$$\frac{\Pi_{i=1}^{p} (\Omega + p_i)}{\Pi_{i=1}^{q} (\Omega + z_i)} = -\nu_{id} < 0. \tag{31}$$

Because the collision frequency is real and positive, we can calculate the complex phase angles of both sides of the latter equation, yielding

$$\sum_{i=1}^{p} \arg(\Omega + p_i) - \sum_{i=1}^{q} \arg(\Omega + z_i) = (2l+1)\pi. \tag{32}$$

Note that Ω is chosen to be real here, p_i is complex, and $\arg(\Omega + p_i)$ stands for the angle between the horizontal axis and the line segment that connects $-p_i$ and Ω. In that geometric interpretation it is easy to see that real p_i located to the left of Ω have no contribution to the left-hand side of Eq. (32); equivalently, it can be seen that a real pole p_i located to the right of Ω has a contribution π. However, complex conjugate poles p_i and p_i^* have no contribution to the left-hand side of Eq. (32) at all, because their phase angles cancel each other out. The interpretation for the zeros is exactly the same, and we can conclude that points of the rootlocus on the real axis lie to the left of an odd number of finite poles and zeros. Phrased equivalently, an interval on the real axis belongs to a rootlocus plot if the sum of the number of poles, located to the right of this interval, and the number of zeros, each also located to the right of this interval, is odd.

Working with the same nomenclature it can be proved that there are $n-m$ asymptotes with center σ, making an angle α with the horizontal axis, where

$$\sigma = -\frac{\Sigma_{i=1}^{p} p_i - \Sigma_{i=1}^{q} z_i}{p - q}, \tag{33}$$

$$\alpha = \frac{(2l+1)\pi}{p - q}, \tag{34}$$

and thus for Eq. (22) the negative real axis will be the only asymptote.

Furthermore, it can be proved that the plot will be horizontal in the poles and zeros. The starting angles in the poles (θ_s) and the ending angles in the zeros (θ_e) can be calculated, using the formulas

TABLE I. Classification for different wave number regions.

k	...	k_Λ	...	k_{cr}	...
Λ	+	0	−	−	−
r_{da}	+	+	+	0	−
Case	C		B		A

$$\theta_s(p_k) = \frac{1}{\mu}\left[(2l+1)\pi + \sum_{j=1}^{q} (z_j - p_k) - \sum_{\substack{i=1 \\ i \neq k}}^{p} (p_i - p_k) \right],$$

$$\theta_e(z_k) = \frac{1}{\mu}\left[(2l+1)\pi + \sum_{i=1}^{p} (p_i - z_k) - \sum_{\substack{j=1 \\ j \neq k}}^{q} (z_j - z_k) \right],$$

where μ stands for the multiplicity of the respective pole or zero. That the plots indeed start and terminate horizontally can be independently checked, starting from Eqs. (24)–(27).

There is another class of important points needed to determine a rootlocus unambiguously; so-called breakaway points are points on the real axis where two or more branches of the rootlocus depart from or arrive at. For the dispersion relation (22) there always is at least one breakaway point, viz., $\Omega = -\sqrt{|r_{ia}|}$. More details about breakaway points are given in the Appendix.

For cold dust, we can make a classification for different configurations, depending on the signs of Λ and r_{da}. For every configuration the poles $\pm i\sqrt{|r_{ia}|}$ are located on the imaginary axis and the origin is a zero. Note that a situation with positive Λ and negative r_{da} is impossible within the assumption $k\lambda_D \ll 1$. After all, negative r_{da} requires $k > k_{cr}$ and thus $\omega_{Jd}/\omega_{pd} < k\lambda_D \ll 1$. Therefore a positive Λ demands $k < k_\Lambda$, but this is impossible since $k > k_{cr} > k_\Lambda$.

For dusty plasmas where the electromagnetic interactions are dominant, i.e., $(1 + n_{i0}Z_i/n_{d0}Z_d)\omega_{pd} > \omega_{Jd}$, there are three regions in wave number space, separated by k_Λ and k_{cr}, as displayed in Table I. We repeat that $k_\Lambda < k_{cr}$, as proved earlier. On the other hand, for dusty plasmas where self-gravitational interactions dominate, i.e., $(1 + n_{i0}Z_i/n_{d0}Z_d)\omega_{pd} < \omega_{Jd}$, the analysis is independent of the wave number and corresponds with case C.

We can qualitatively describe how the magnitude of the dust-ion collision frequency affects the real frequency and damping decrement of the Jeans and ion-acoustic modes by plotting the rootlocus in the possible configurations.

A. $\Lambda < 0$, $r_{da} < 0$

This situation corresponds to dusty plasmas for which self-gravitational interactions do not prevail, viz., $(1 + n_{i0}Z_i/n_{d0}Z_d)\omega_{pd} > \omega_{Jd}$, and for wave numbers exceeding the critical wave number, $k > k_{cr} = \omega_{Jd}/c_{da}$. The second condition is stronger than the first condition because, if $\omega_{Jd}/\omega_{pd} < k\lambda_D \ll 1$, the first condition is automatically satisfied. We can conclude that this category is the category of dusty plasmas with negligible self-gravitational interactions, i.e., $\omega_{Jd} \ll \omega_{pd}$.

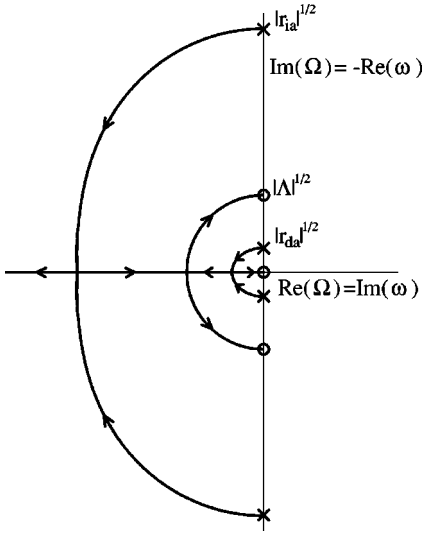

FIG. 1. Rootlocus plot for wave numbers $k>\omega_{Jd}/c_{da}$. The crosses and circles correspond to, respectively, the poles and zeros of $\Omega(\Omega^2-\Lambda)/(\Omega^2-r_{ia})(\Omega^2-r_{da})$, whereas the arrows are directed towards larger collision frequencies.

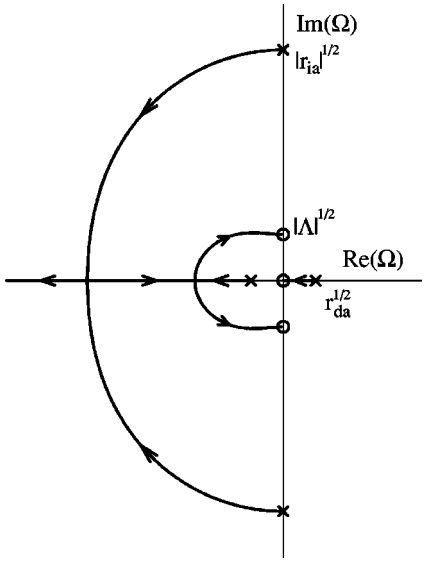

FIG. 2. Rootlocus plot for dusty plasmas with $\omega_{pd}>\omega_{Jd}$ and corresponding to wave numbers $k_\Lambda<k<k_{cr}$.

For this case, all poles and zeros of Eq. (22) are located on the imaginary axis and alternate because here $|r_{da}|<|\Lambda| \ll|r_{ia}|$, as can be seen in Eq. (23). It can easily be seen now that the entire negative real axis is part of the rootlocus plot and it also can be proved that the rootlocus plot leaves from the poles perpendicularly to the imaginary axis and directed towards the left half of the complex plane. Equivalently it can be shown that the rootlocus plot arrives in the zeros, perpendicular with the imaginary axis and coming from the left half of the complex plane. As stated earlier, the plot cannot cross the imaginary axis except in the poles or zeros; therefore, this configuration is always stable, since the rootlocus plot is entirely located in the left half of the complex plane. This confirms the results of D'Angelo [6], albeit in a more general way.

Note that statements about the stability of the system have been made with a minimal use of rootlocus theory and without the need of a plot. It is only for a qualitative determination of the real frequencies and damping decrements that a rootlocus plot has to be made. Qualitative and quantitative results can be found easily and rapidly for numerical examples, using existing routines, but analytical expressions can also be dealt with in a qualitative way, as is shown further on.

For configurations with $|r_{da}|<|\Lambda|<9|r_{da}|$, the rootlocus can have multiple possibilities depending on the precise magnitude of the parameters; i.e., the number of breakaway points cannot easily be determined without additional specification of the magnitudes of r_{ia}, r_{da}, and Λ, and therefore a general plot is not given. For configurations $9|r_{da}|<|\Lambda|$, there are three breakaway points and the rootlocus plot is shown in Fig. 1. Details about the determination of the number of breakaway points are given in the Appendix.

Figure 1 shows that dust-acoustic and ion-acoustic modes initially reduce in real frequency and become damped. As the collision frequency increases they become zero-frequency modes; subsequently, one of the ion-acoustic modes becomes completely damped while one of the dust-acoustic modes also vanishes as it becomes zero. The remaining dust-acoustic and ion-acoustic modes couple and leave the real axis again for high collision frequencies. If one plots discrete points, corresponding to fixed collision frequencies, one can see that initially (for collision frequencies that are not too large) the modes do not deviate much from their respective collisionless limits.

B. $\Lambda<0$, $r_{da}>0$

This situation also corresponds to dusty plasmas for which self-gravitation is not having the upper hand or, equivalently, $(1+n_{i0}Z_i/n_{d0}Z_d)\omega_{pd}>\omega_{Jd}$, but now corresponds to the wave number region $k_\Lambda<k<k_{cr}$.

In this configuration there are two poles ($\pm\sqrt{r_{da}}$) located on the real axis; the remaining two poles ($\pm i\sqrt{|r_{ia}|}$) are located on the imaginary axis as are all zeros ($0,\pm i\sqrt{|\Lambda|}$). The intervals $[-\infty,-\sqrt{r_{da}}]$ and $[0,\sqrt{r_{da}}]$ of the real axis are part of the rootlocus plot; obviously, this means that this configuration is always unstable.

The plot leaves the poles $\pm i\sqrt{|r_{ia}|}$ towards the left and perpendicular to the imaginary axis, and arrives in the zeros $\pm i\sqrt{|\Lambda|}$ from the left and also perpendicular with the imaginary axis. As ν_{id} increases, the unstable dust-acoustic root $\sqrt{r_{da}}$ moves over the real axis towards the origin and hence instability remains, but the growth rate diminishes.

The rootlocus plot of dusty plasmas in this category is shown in Fig 2. It shows that the growth rate of the unstable Jeans mode indeed reduces with increasing collision frequencies; the stable Jeans mode and the ion-acoustic modes are also damped initially while their real frequency diminishes. For larger collision frequencies the ion-acoustic roots become zero-frequency modes and there is bifurcation on the real axis; one mode becomes completely damped while the other couples with the stable dust-acoustic mode and both

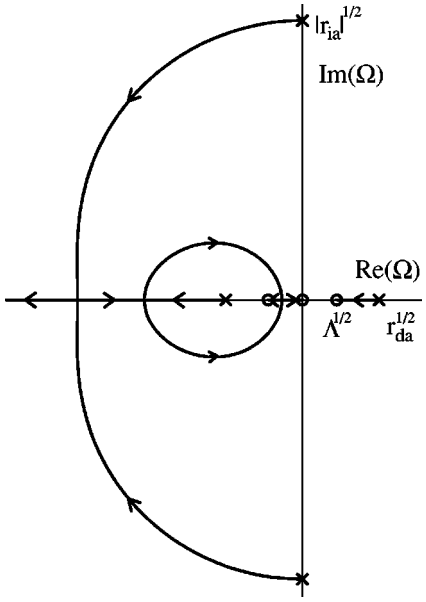

FIG. 3. Rootlocus plot for dusty plasmas with dominating self-gravitational effects and also for the wave number region $k<k_\Lambda$ in dusty plasmas with relatively light dust species ($\omega_{pd}>\omega_{Jd}$).

eventually leave the real axis again.

C. $\Lambda>0$, $r_{da}>0$

There are two different classes of dusty plasmas residing in this category. On the one hand, dusty plasmas with relatively light dust species that obey $(1+n_{i0}Z_i/n_{d0}Z_d)\omega_{pd}>\omega_{Jd}$ and in a situation $k<k_\Lambda$. On the other hand, dusty plasmas where self-gravitation predominates, i.e., $(1+n_{i0}Z_i/n_{d0}Z_d)\omega_{pd}<\omega_{Jd}$, since $k\lambda_D\ll 1$ the inequality $k<k_{cr}=\omega_{Jd}/(\omega_{pd}\lambda_D)$ is always satisfied for this case. Note that the quantity k_Λ is meaningless in the latter situation as Λ is positive over the entire wave number range.

Both classes have qualitatively similar plots. The zeros are located on the real axis as are the poles $\pm\sqrt{r_{da}}$. The poles are always larger (in absolute value) than the zeros since Eq. (23) demonstrates $\Lambda<|r_{ia}|,r_{da}$. The real intervals $[-\infty,-\sqrt{r_{da}}]$, $[-\sqrt{\Lambda},0]$, and $[\sqrt{\Lambda},\sqrt{r_{da}}]$ belong to the rootlocus plot, rendering also this configuration unstable. Again, starting and ending angles are perpendicular to the imaginary axis; the larger poles leave toward the left half of the complex plane, while the smaller ones arrive along the axis in $\sqrt{\Lambda}$.

The rootlocus plot is shown in Fig. 3. The growth rate of the unstable Jeans mode also reduces until it reaches the pole $\sqrt{\Lambda}$. Here one of the ion-acoustic modes will also couple with the stable dust-acoustic mode while the other is wiped out. Note that the only difference with the previous case is the evolution for large collision frequencies and the evolution of the unstable root. Namely, in this class of dusty plasmas the unstable root improves but will never be stable, as ν_{id} increases.

V. CONCLUSIONS

The stability of longitudinal disturbances in self-gravitating dusty plasmas has been investigated previously within a collisionless model. We studied the modifications for the stability analysis if dust-ion collisions are included. We also illustrate qualitatively how the real frequency and damping decrement of the ion-acoustic and Jeans modes change over the spectrum of possible collision frequencies, using a semianalytical method called rootlocus. This method, often used in control engineering, proves to be an enlightening tool for the stability analysis of our model as it can produce physically meaningful graphs.

It shows that dust-ion collisions reduce the growth rate of the unstable Jeans dust mode but can never overturn the gravitational instability.

On the other hand, the ion-acoustic modes are also damped and can become zero-frequency modes when the collision frequency exceeds a certain threshold. As the inclusion of self-gravitational effects hardly modifies the ion-acoustic modes, the results of Ivlev *et al.* [10] are partly reproduced and in some way generalized for the ion-acoustic branch.

ACKNOWLEDGMENTS

G.J. and F.V. acknowledge a research grant from the Bijzonder Onderzoeksfonds of the Universiteit Gent. V.V.Y. thanks the "Onderzoeksfonds K.U. Leuven" for support (Grant No. F/00/070).

APPENDIX: BREAKAWAY POINTS

Breakaway points b_i of multiplicity μ (μ branches depart and μ branches arrive) are formally calculated as solutions of

$$\left[\frac{d^j}{d\Omega^j}\frac{N(\Omega)}{D(\Omega)}\right]_{b_i}=0 \quad \forall j=1,\ldots,\mu-1, \tag{A1}$$

which of course still obey $D(\Omega)+\nu_{id}N(\Omega)=0$. Breakaway points b_i of the dispersion relation (22) are hence solutions of

$$\begin{aligned}\Omega^6+(r_{ia}+r_{da}-3\Lambda)\Omega^4+[\Lambda(r_{ia}+r_{da})-3r_{ia}r_{da}]\Omega^2\\ +r_{ia}r_{da}\Lambda\simeq\Omega^6+r_{ia}\Omega^4+r_{ia}(\Lambda-3r_{da})\Omega^2\\ +r_{ia}r_{da}\Lambda=0,\end{aligned} \tag{A2}$$

with corresponding collision frequency

$$\nu_{id}=-\frac{b_i^4-b_i^2(r_{ia}+r_{da})+r_{ia}r_{da}}{b_i(b_i^2-\Lambda)}. \tag{A3}$$

There is always one negative breakaway point, approximated using the obvious inequalities $r_{da},\Lambda\ll r_{ia}$, as

$$(b_1, \nu_{id}) = (-\sqrt{-r_{ia}}, 2\sqrt{-r_{ia}});$$

this is the only breakaway point for case *A* if $|\Lambda| < 9|r_{da}|$. Other possible breakaway points are b_2 and b_3, where

$$\Omega = b_{2,3} = -\sqrt{\frac{1}{2}[3r_{da} - \Lambda \pm \sqrt{(\Lambda - r_{da})(\Lambda - 9r_{da})}]},$$

with corresponding real and positive collision frequencies

$$\nu_{id} \simeq -r_{ia} \frac{(r_{da} - b_{2,3}^2)}{b_{2,3}(b_{2,3}^2 - \Lambda)}.$$

For cases *A* (if $9|r_{da}| < |\Lambda|$), *B*, and *C*, b_2 is indeed a second breakaway point; additionally, for cases *A* ($9|r_{da}| < |\Lambda|$) and *C*, b_3 represents a third breakaway point.

[1] N.N. Rao, P.K. Shukla, and M.Y. Yu, Planet. Space Sci. **38**, 543 (1990).

[2] P. Bliokh, V. Sinitsin, and V. Yaroshenko, *Dusty and Self-Gravitational Plasmas in Space* (Kluwer, Dordrecht, 1995).

[3] F. Verheest, *Waves in Dusty Space Plasmas* (Kluwer, Dordrecht, 2000).

[4] P.K. Shukla and A.A. Mamun, *Introduction to Dusty Plasma Physics* (Institute of Physics, Bristol, 2002).

[5] F. Verheest, G. Jacobs, and V. Yaroshenko, Phys. Plasmas **7**, 3004 (2000).

[6] N. D'Angelo, Phys. Plasmas **5**, 3155 (1998).

[7] K.N. Ostrikov, S.V. Vladimirov, M.Y. Yu, and G.E. Morfill, Phys. Rev. E **61**, 4315 (2000).

[8] P.K. Shukla, M.R. Amin, and G.E. Morfill, Phys. Scr. **59**, 389 (1999).

[9] D. Winske and M. Rosenberg, IEEE Trans. Plasma Sci. **26**, 92 (1998).

[10] A.V. Ivlev, D. Samsonov, J. Goree, and G. Morfill, Phys. Plasmas **6**, 741 (1999).

[11] P.K. Shukla and F. Verheest, Astrophys. Space Sci. **262**, 157 (1999).

[12] P. Meuris, F. Verheest, and G.S. Lakhina, Planet. Space Sci. **45**, 449 (1997).

[13] J. Willems, *Stability Theory of Dynamical Systems* (Nelson and Sons, London, 1970).